6th International Conference on Water Resources and Arid Environments (ICWRAE 6): 401-419
16-17 December, 2014, Riyadh, Saudi Arabia

Optimal Management of Groundwater Resources in Arid Areas Case Study: North Sinai, Egypt

[1]M.I. Gad, [2]S.A.M. Zeid, [3]S. Khalaf, [4]A.M. Abdel-Hamid, [2]E.M. Seleem and [5]A. El Feki

[1]Mathematical Modeling Unit, Hydrology Division, Desert Research Center, Cairo, Egypt
[2]Geology Division, Faculty of Science, Al-Azhar University, (Assiut Branch), Egypt
[3]Irrigation and Hydraulics Department, Faculty of Engineering, Mansoura University, Egypt
[4]Hydraulic Research Institute, National Water Research Center, Cairo, Egypt
[5]Department of Hydrology and Water Resources Management, KAU, Jeddah, KSA

Abstract: The groundwater resources in North Sinai area are affected by salt water up-coning due to over-pumping phenomenon beside seawater intrusion. To protect these salt-affected ecosystems, an optimum water resources management is carried out by applying mathematical modeling techniques in this paper. The chosen area for study is located in the northern coastal zone of Sinai Peninsula of Egypt and covers about 1750 km^2. It is bounded by the Mediterranean Sea to the North and Gebel El-Maghara and Arish-Rafah highway to the south. Its climate is hot in summer and rainy in winter. Field investigations show that the Quaternary Aquifer in the North Sinai Area (QANSA) is highly affected by salt water up-coning due to over-pumping phenomenon beside seawater intrusion. El Arish airport area, El-Maazar village, El-Taweel village and El-Kharouba area are greatly affected by the groundwater level decline which reaches 15 m at its maximum value. The methodological approach to simulate the groundwater flow is based on the mathematical modeling techniques applying 3D finite element software (FEFLOW model). The total surface area of the model domain reaches 600 km^2. The two aquifer zones are discretized into 2 layers and 3 slices. Three management scenarios are applied to detect the future predictions in the drawdown of groundwater levels under different extraction rates and seawater intrusion phenomenon. In addition, the methodology of seawater intrusion study is based on applying two-dimensional finite element simulation algorithm (SINM) depending on the calibrated outputs of the MODFLOW code. The results of groundwater flow simulation show optimum groundwater extractions of 26 million m^3/year from the cultivated areas. Moreover, Simulation results indicate that the seawater/freshwater interface will migrate, after 15 years, 5.5 Km landward from its initial position if the present groundwater production policy (19 million m^3/yr) continues operating in the investigated area. The predicted interface toe positions will migrate 13 Km from its initial position after 15 years in case of increasing the groundwater production by 4%. While the climate change will cause its migration by 5.3 Km landward from its initial position assuming a rise of sea water level by 0.5m. To conserve the QANSA storage for longer time, it is recommended to reduce the number of the pumping wells (less than 300 wells), reduce the initial and running time (does not exceed 10 hours) and achieving the objective of implementing the developing policy without any increase (500 m^3/day/well). Otherwise, to mitigate the migration of the interface toe position, subsurface flow toward sea of 144443 m^3/day is needed. It is highly recommended to carry out geophysical exploration study and constructing monitoring network to verify the results of the applied model.

Key words: Hydrogeology ▪ Optimal management ▪ FEFLOW and SINM codes ▪ North Sinai

INTRODUCTION

In arid and semiarid ecosystems, recharge fluxes are often very small percentage of the total precipitation falling over the basin and highly heterogeneous in space and time [1]. The quality of groundwater is of equal importance in many arid and semiarid ecosystems, where the impacts and chemical processes related to salinization often represent the single largest threat to freshwater resources [2]. A common mechanism of groundwater

Corresponding Author: Mohamed I. GAD, Hydrology Division, Desert Research Center, Egypt.

salinization in areas of freshwater pumping is induced migration of local naturally occurring brackish, saline groundwater or seawater [3]. In areas susceptible to pumping-induced salinization, a diffuse mixing layer of variable thickness separates fresh and brackish groundwater. When freshwater sections are pumped, the positions of nearby mixing zones are affected directly and, if pumping rates are high enough, saline water may even move into the well-capture zone, resulting in contamination [4].

The aim of this paper is to predict the future change in the groundwater quality and quantity in the Quaternary Aquifer in North Sinai coastal Area (QANSA) under different water polices beside the seawater intrusion as a tool to shed a light on the optimum groundwater management in salt-affected ecosystems in North Sinai coastal area.

Site Description: The Sinai Peninsula occupies an area of about 61,000 Km^2. The study area is located in the northeastern part of Egypt (Fig. 1). The importance of the Sinai is referred to its location, where it constitutes the eastern border of Egypt and the first defense line. Therefore, it must be done what is called the population development which depends on the development, economy, education, agriculture…etc. The groundwater is the main source for agricultural, municipal, domestic and drinking purposes.

The expansion of the economy of Sinai, beside the rapid growth of its population in the last decade, has increased the water demands. The groundwater supply in the Sinai Peninsula is generally insufficient to meet the predicted increase in water demands. Accordingly, serious strategies for water development have been established to fully utilize the surface and groundwater resources at economic costs. Recently, the Sinai Peninsula has received great attention in respect to future agricultural development, especially after initiation of El Salam canal to the northern coastal area, as a source of irrigation water. Therefore, a detailed groundwater investigation was undertaken to elucidate the principal hydrogeological and hydrogeochemical aspects of the northeastern part of Sinai. The average annual rainfall is about 140 mm at El Arish. The average temperature is 27°C in summer, while in winter is 15°C. Evaporation plays a principal role in the groundwater regime; they affect both the groundwater quantity and quality. The maximum mean monthly evaporation is about 17 mm/ day in June (at El Maghara), while it is 5 mm/d in September at El Arish [5]. The total evaporation decreases generally in the northeastern direction, i.e. towards El Arish and Rafah, while it increases due El Qantara –El Massaid (the investigated area about 100 mm/y).

Geomorphological Features: The area under investigation is characterized by moderate relief with elevations varying from about sea level to less than 1000 m. The present landforms are developed as a result of the endogenetic and the exogenetic processes. According to [6] this region morphologically can be subdivided into six units (Fig. 2). El Halal-El Amer Tilted Blocks are series of anticlinal ridges arranged and oriented in a NE - SW direction. Such ridges are represented by EI Halal (921m asl), EI Dalfa (405m asl) and EI Amer (474m asl). This arc also represented by a series of smaller ridges which include Gebel Libni (463m asl), Gebel Risan Aneiza (370m asl) to the west of the area and Gebel Taret um Basis (260m asl) to the south. All such ridges are underlain by weathered dolometic rocks. They also, represent conspicuous water- shed area. Between the anticlinal ridges, there are shallow synclinal basins, which form important accumulation for water, where deposition of modern alluvial and aeolian deposits takes place. El Rawafaa-El Auga Foot slopes between El Halal-El Amer anticlinal ridges consider a transitional zone (200m asl) which has a width exceeding 5 km. In this zone, the surface is underlain by soft Cretaceous and Eocene rocks which lack of sharp relief. The surface of this zone is occasionally covered by down wash deposits. El Gora-El Massaied Old Coastal plain lays northward from the upland area and its foot slopes. This vast pediment plain extends to the modern coastal belt of Mediterranean Sea, i.e., over a distance of 50 km. It has surface with gentle slopes in the northward (2m/km). On the regional view, this plain occupies a portion of a great morphotectonic depression which contains the alluvial deposits. Port Said-Rafah Coastal Belt is parallel to the shoreline as a series of foreshore dune ridges. In this belt, modern beaches as well as old are of broad undulations of the surface. It has a length of about 50 km, a width of about 4 km and the ground elevation is about 30m asl. In this belt the surface is distinguished into a variety of landforms which include, the sand dune ridges, the old flood plains, the raised beaches (10m asl) and the modern beaches which extend along El Arish-Rafah with average width 500m. Drainage basins are bounded from the west by wadi EI Arish and dissected by several wadis e.g. Al Azaric, Haredien, El Mazar and El Kharuba. These drainage basins are controlled by the local tectonic and lithologic feature. The trunk channels of the majority drainage basins owe their origin to WNW - ESE faults.

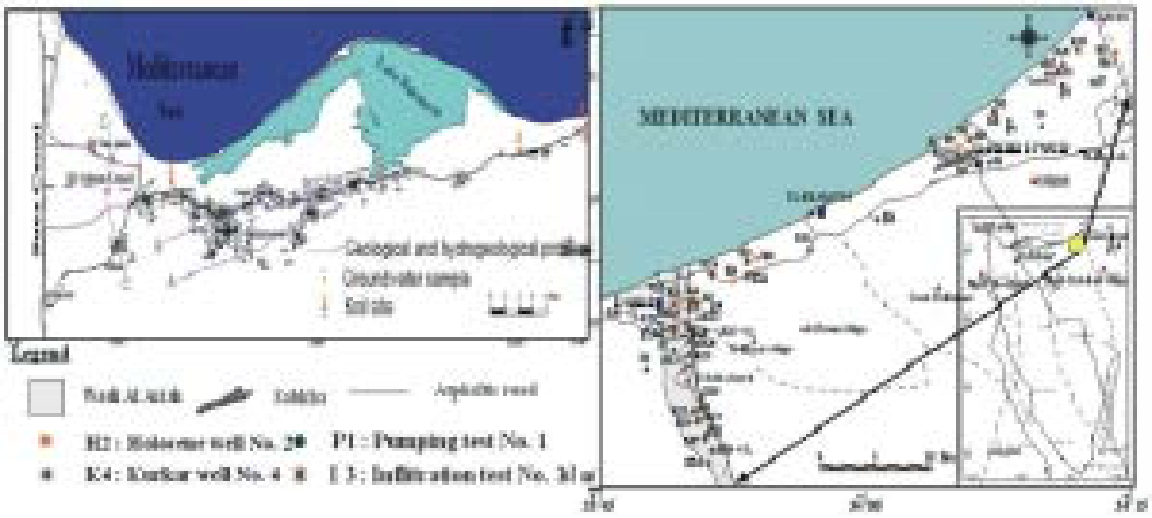

Fig. 1: Location map of the study area showing the operating wells in the eastern part (left map) and in the western part (right map) of the QANSA

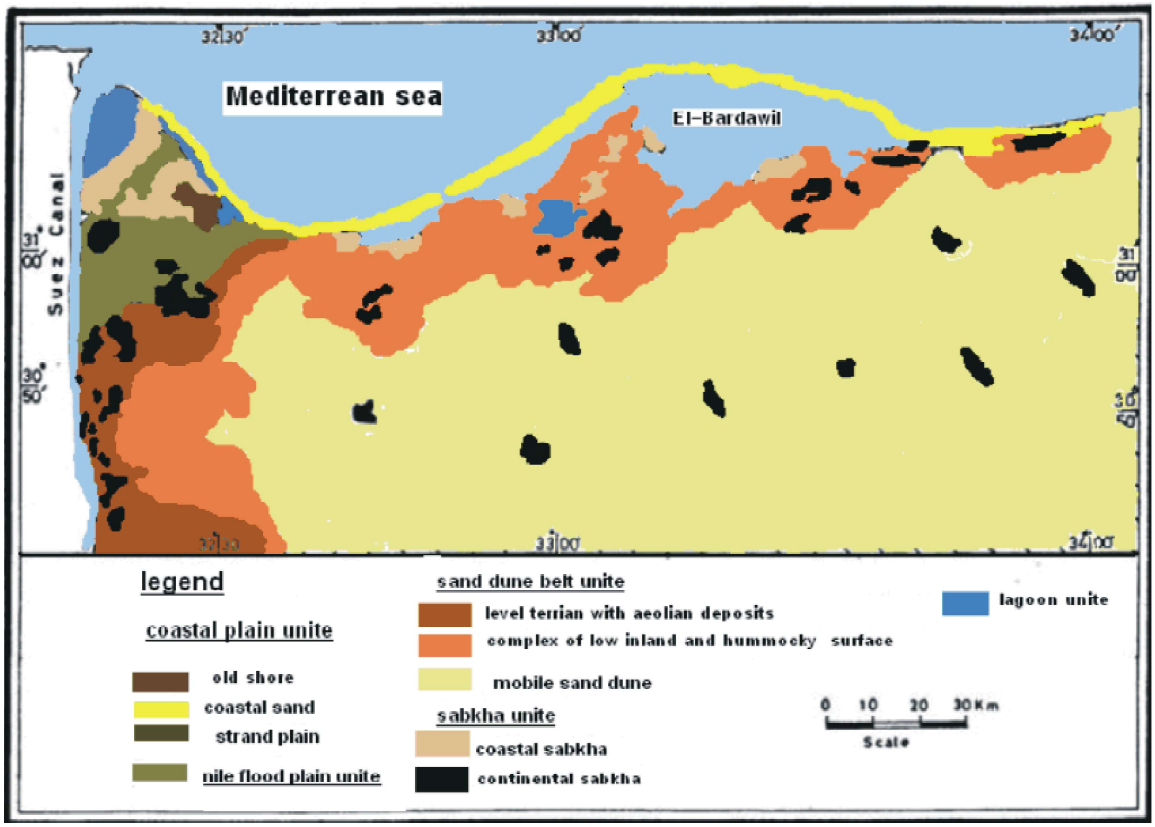

Fig. 2: Geomorphologic map of the western part of QANSA

Salt marsh (Sabkha) is represented near the shore of the Mediterranean Sea at EI Sheik Zuwayid, where it is formed in the area below sea level. The Sabkha is formed due to seawater intrusion as well as the discharge of ground water in this part.

Geological Setting: The exposed sedimentary rocks in the North Sinai area belong to the Triassic to Quaternary ages [7, 8, 9, 10, 11, 12, 13] (Fig. 3). The Triassic rocks in the North Sinai are exposed in the core of Gebel Arief El-Naqa anticline. These deposits have average thickness

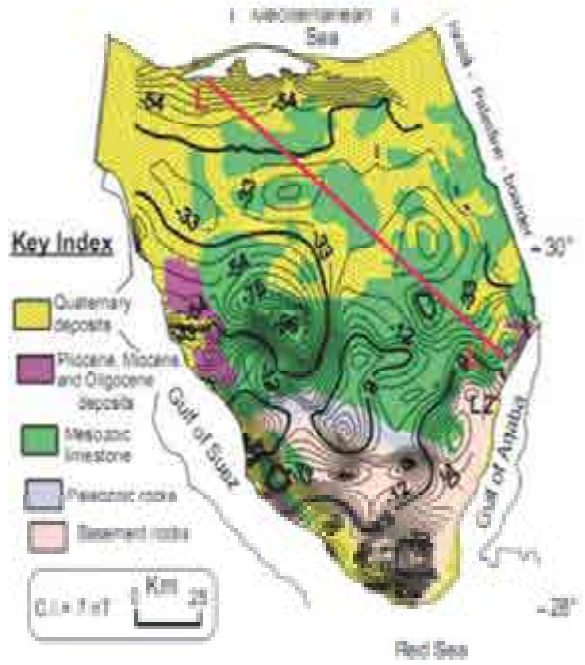

Fig. 3: Geological map of Sinai Peninsula (compiled from different authors)

of 200 m and composed of sandstone and shale with limestone intercalation. They are overlain by the Cretaceous and Eocene rocks. The Jurassic rocks are exposed in northern Sinai in Gebel EI Maghara (2000m thick), Gebel Risan Aneiza and Gebel Minsherah. These deposits are overlain by the lower and Upper Cretaceous rocks. The Cretaceous rocks are well represented in Gebel El Halal, Gebel Yelleg, Gebel Libni, the greater part of Gebel Risan Aneiza and considerable part of Gebel EI Maghara. The Cretaceous deposits are classified into the Lower (thick deposits of sandstone intercalated with shales, limestone and marl beds with thickness of more than 520m) and the Upper Cretaceous which includes the Cenomanian (limestone and dolomitic beds with relatively small intercalation of sandstone and shale with thickness ranges from 320 to 520m), Turonian (hard dolomitized with some flint hands thickness about 100m in Gebel El-Halal) and Santonian rocks which consist of marly limestone with chalky limestone interbeds. The Paleocene sediments are represented by the Esna Shale Formation. They are observed at many localities such as El Maghara (65 m thick), Arief El Naqa (50 m) and El Qusaima area (13 m thick).The Eocene deposits form the vast synclinal areas between Gebel El Halal and Yelleg and between Gebel El Maghara and Yelleg. In the subsurface, the three series of the Eocene deposits are detected in El Khabra, El Amr, Um Shehan, Misri-l and Road-l wells with thickness ranging from 177 to 301 m. The Oligocene rocks are represented by basaltic intrusions, where the most noticeable are dykes. These dykes are detected in wadi El Hamma (El Maghara basin) and in wadi El Hassana; and they are oriented the NW-SE direction [12]. The Miocene rocks are exposed at Awlad Ali and Risan Aneiza. They consist of interbedded sequence of marl, marly limestone and shale. The maximum exposed thickness is determined at Awlad Ali (about 15 m).

The Pliocene deposits are exposed in one locality along the channel of wadi El Arish at Awlad Ali - Maqdaba. They are distinguished into the Upper conglomerate series (3 to 5m thick and is overlain by the marine Kurkar and underlain by the Pliocene marl deposits) and the lower marl series which are exposed in Awlad Ali and EI Maqdaba. At Awlad Ali, the deposits are composed of yellow and gray sandy marl with thickness of about 8 m. The Pleistocene deposits have a wide distribution. They are divided into the Lower Pleistocene deposits (about 40 m thick) and the Upper one (Alluvium deposits and old beach deposits). The Holocene deposits have a wide distribution in the study area. These are developed into variety of formations such as sand dunes, modern beach deposits, alluvial and lagoonal deposits. Salinas are Marshy deposits which have limited distribution in the area of study. They are particularly noted at El Sheik Zuwayid (Sabkht El Sheikh Zuwayid). These deposits are made up of evaporates and occasionally mixed with detrital materials.

Hydrogeological Setting: The water bearing formations include the most fresh groundwater resource in the QANSA and the brackish Pliocene aquifer. In the eastern coastal part (Fig. 4-A), QANSA consists of sand dunes, old beach sand and the Kurkar (calcareous sandstone) formations. The thickness of this QANSA ranges from 80 to 100m [14]. In the western coastal part (Fig.4-B), the QANSA (Holocene and Pleistocene) thickness varies from 150 m (Bir El Abd well) to 330 m (Qatia-1 well) and rests directly on the Pliocene clay. According to [16, 5, 15], the groundwater in the south of Lake Bardawil (western part) is tapped from different water bearing formations, which are Holocene and Pleistocene.

The Holocene sand aquifer in the studied area is developed along the coastal plain from Gilbana to El Massaid along a distance of about 150 km with average width 20 km in the form of elongated sand dunes (coastal) or sand sheet (inland) or saline sand (sabkhas). On the other hand, this aquifer wedges out at El Tina plain until it vanished. The groundwater of the Holocene aquifer exists under free water table condition, where depth to

Fig. 4-A: Hydrogeological cross-section showing the aquifer systems in the western part of QANSA after [38]

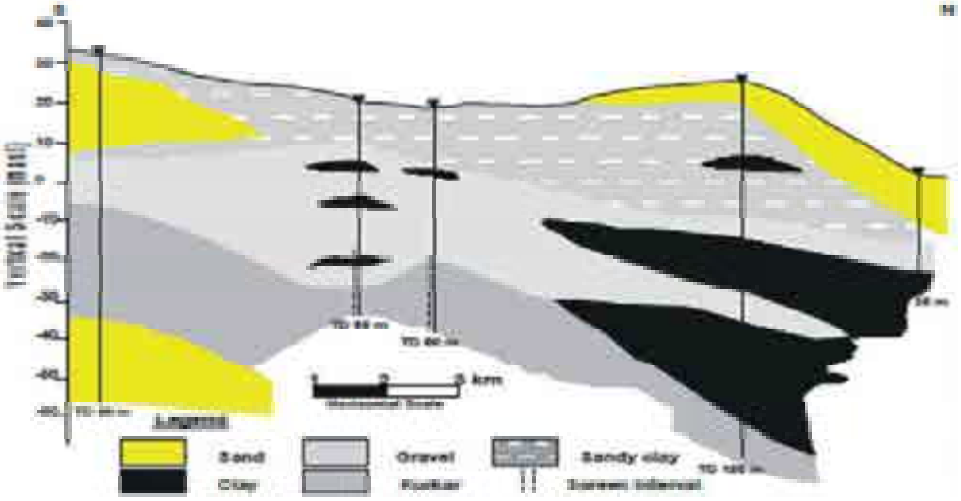

Fig. 4B: Hydrogeological cross-section showing the aquifer systems in the eastern part of the study area (El -Arish-Rafah) after [21]

water ranges from 2 to 10m below ground surface. However, this depth is very near to the ground surface close to the sea shore. The infiltration and percolation from direct rainfall and surface runoff is the main source of recharge in the aquifer.

The alluvium aquifer (Pleistocene) is commonly composed of sands and gravels with intrusion of silt and clay. Due to the capability of the alluvial deposits to store and transmit groundwater, the alluvium aquifer represents one of the most productive aquifers in the studied area. Rainfall intensity greatly affects the rate of recharge of such aquifer. In El Tina plain, the groundwater comes very near to the ground surface. The depth to water varies from less than one meter at north to about 2 m at south as a result of the presence of cap rock (30 m clay),where such aquifer in El Tina plain area is confined [15]. To the southern part of El Tina Plain (East El Qantara), the Pleistocene aquifer is about 170 m thickness and it rests directly on the Pliocene aquiclude, where both the Holocene and Pleistocene aquifers are partially hydrogeologically interconnected [15]. On other hand, in Qatia area, the Pleistocene aquifer attains about 300 m in thickness due to presence of graben structure [12].

The water table level in the QANSA ranges between less than 2 m at El Tina plain to 12 m at the coastal area at El Medan. The regional groundwater flow is directed towards north (Fig. 5-lower right), locally towards NW (El Tina Plain) and northeast (Fig. 5-upper), where the recharge area is the mountains of Gabel El Maghara, which lie in southern part of the study area. The overlap of water table in 1998 and present work yield change in water table map (resultant map Fig. 5-lower left). It is noticed that the areas of rising water table level, (from 1 to 6 m), are around El Salam canal (Baloza, El Ahrar, Qatia, Kasraweet, El Nasr and Kherba) where the rate of recharge exceeds that of the discharge. Moreover, the areas of groundwater depletion (over-pumping zone) presents at south of El Qantara and El Kasraweet areas. They refers to water extraction more than the recharge; while Kherba, Negila and Gilbana areas are characterized by constant water level, where the withdrawals are nearly equal to the recharge.

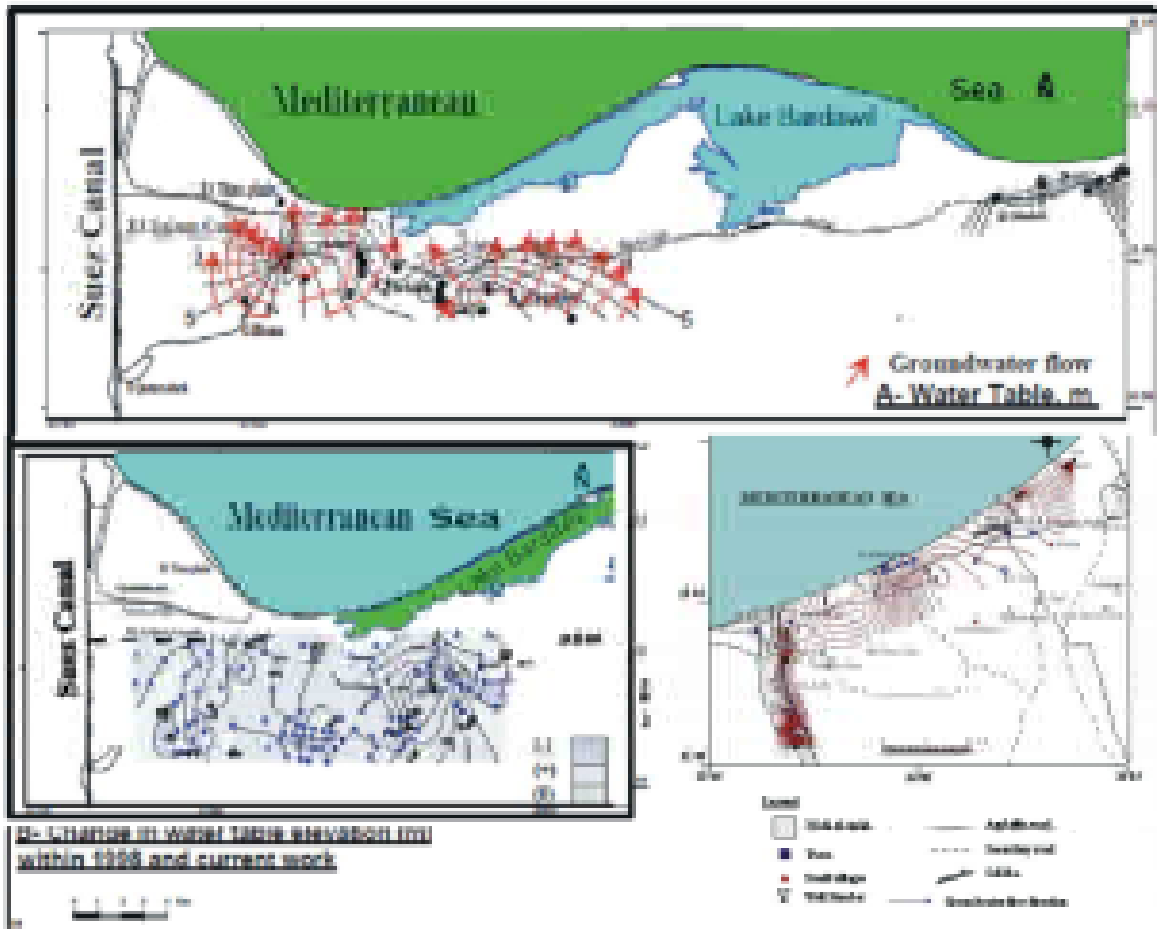

Fig. 5: Water table map for the western part (upper) and eastern part (lower right) and Resultant map (lower left-after [38]) for QANSA

MATERIALS AND METHODS

The materials used in this paper covered both collecting groundwater intake database and water sampling for physical and chemical analyses. Groundwater database included collection of archival data (such as well drilling reports), registration of discharge, distribution of wells, piezometeric heads and recording potential sources for quality changes. Number of 21 water samples representing the present three water-bearing formations was sampled from domestic groundwater intake in the QANSA. Chemical analyses were run according to the standard analytical methods in the central laboratory of the Desert Research Center. The location of these wells was given in Figure 1 and the water level records of 18 wells during October 2006 (m asl) and both total dissolved solids (TDS in mg/l) and chloride concentration in mg/l at September 2006 and September 2008 were tabulated in Table 1.

The behavior of fresh-salt water contact in El-Arish area (eastern part of QANSA) at Sep. 1962 was traced according to [17] (Fig. 6). The salinities of selected groundwater samples were compared with the historical data sited in [18, 19, 20] via a transverse profile in N-S direction to determine the deterioration of the groundwater salinity of this part of QANSA (Delta Wadi El-Arish locality) and to form a background for further assessment of seawater intrusion (Fig. 6). Moreover, the groundwater recharge from rainfall was estimated 10% of the average annual rainfall of 140 mm/year [21]. The estimated average recharge from 200 km^2 recharge areas of this eastern part of QANSA reached 22,240 m^3/d [22] or 27,000 m^3/d [23]. Otherwise, sewage effluent constituted an additional source of recharge along El-Arish city center, where about 50,000 m^3/d of the total sewage volume of the city (60,000m^3/d) drained to the groundwater via the poorly developed septic tanks and house gardens [24]. In this study, the recharge rate to the

Table 1: Records of the groundwater levels (masl) and the results of the chemical analysis of the selected samples in the eastern part of the QANSA

				Records of Sept.2006 (m)			Records of Sept.2008 (mg/l)		Records of Sept.2006 (mg/l)	
Serial No	Well name	Longitude	Latitude	GE	DTW	WL	TDS	Cl	TDS	Cl
1	Maghool 1	33.84	31.06	40.1	42	-1.9	2722	1028	---	---
2	Beer El-Magles	33.86	31.15	56	62	-6	2925	1427	---	---
3	Salm Eid Gomaa	33.84	31.13	31.7	40	-8.3	3016	1454	---	---
4	Abdo Sallam 1	33.86	31.03	55.2	65	-9.8	3185	1613	---	---
5	Atef Solim	33.85	31.07	55.7	50	5.7	3435	1507	3683	1775
6	Batn El-Gabl	33.84	31.02	48.2	40.8	7.4	3530	1702	---	---
7	Magles	33.84	31.12	38.6	32.5	6.1	3617	1773	---	---
8	El-Rai37	33.85	31.04	44.8	50.8	-6.02	3627	1702	3906	1985
9	Nassar Farm	33.84	31.06	38.3	36.9	1.4	3799	1596	---	---
10	Abdo Sallam 2	33.86	31.03	45.2	66	-20.8	3820	1972	---	---
11	El-Rai 38	33.85	31.04	43.7	50.8	-7.12	3903	1844	3985	1868
12	Atef solim 2	33.85	31.07	55.7	50	5.7	3994	2172	4288	2585
13	Maghool2	33.84	31.06	41.6	42	-0.4	4051	1844	5056	1925
14	Well 34	33.84	31.10	48.7	61	-12.3	4255	2039	---	---
15	Awwad Farm	33.84	31.06	35.5	36.9	-1.4	1515	650	---	---
16	Tameer-8	33.83	31.12	21.9	18.9	3	3700	2083	---	---
17	Abu Aiman Farm	33.88	31.15	22.3	22	0.3	4879	2482	---	---
18	Cousin -Ibrahim	33.85	31.05	41.8	40	1.8	5181	2704	5117	2735
19	Well 1	33.84	31.11	---	---	---	5185	2527	---	---
20	Well 2	33.82	31.12	---	---	---	5246	2482	---	---
21	Well 3	33.82	31.11	---	---	---	5574	2748	---	---

Note: GE=Ground elevation (m asl), DTW = Depth to groundwater (m), WL = Absolute groundwater level (m asl), TDS = Total dissolved salts in mg/l and Cl = concentration of chloride in groundwater in mg/l

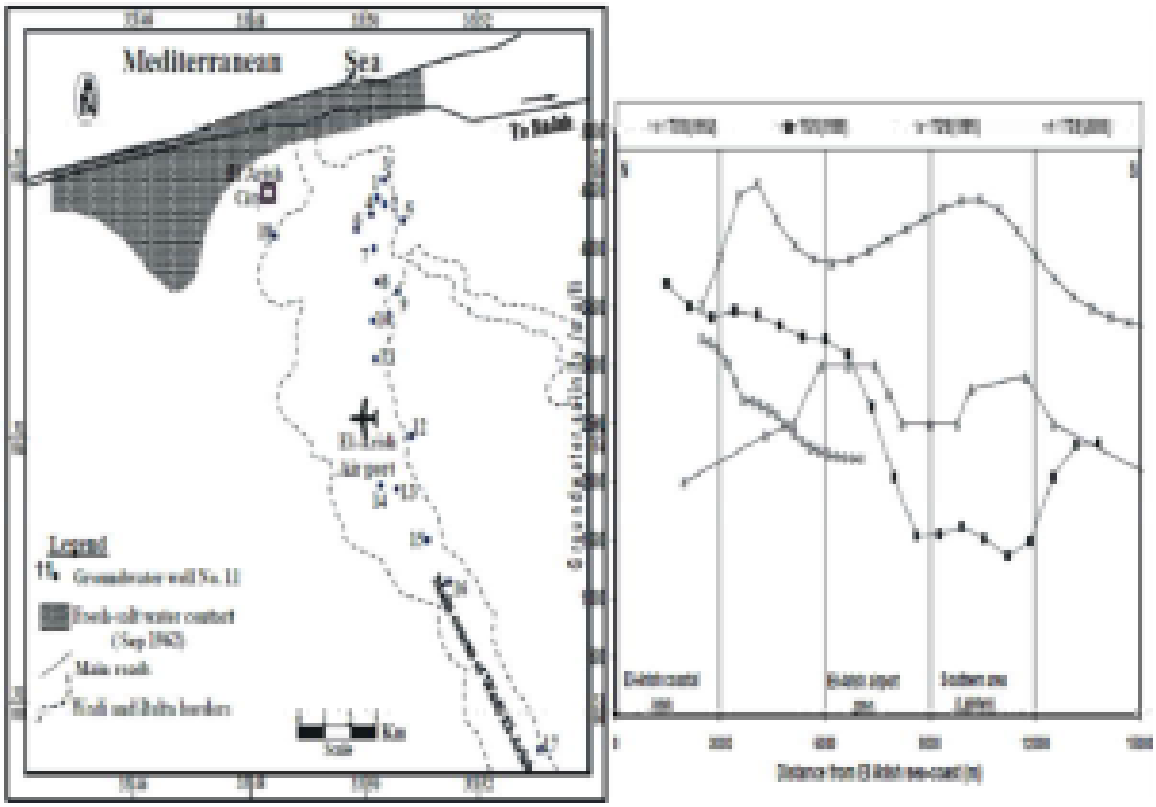

Fig. 6: Fresh-salt water contact in El-Arish area at September 1962 (left map-after [17] and the spatial and temporal changes in groundwater salinity in the eastern part of QANSA

Table 2: The hydraulic parameters and soil infiltration rate of the eastern part of QANSA

	Location							
	Long.	Lat.	Pumping T (m^2/day)	Recovery T (m^2/day)	Average T (m^2/day)	S	Diffusivitym^2/day	Infiltration rate (m/day)
P1	33.79	31.11	489	391	440	0.068	6471	15.78
P2	33.82	31.1	183	232	208	0.08	2600	26.06
P3	33.79	31.09	429	507	468	-----	-----	10.44
P4	34.07	31.23	93	534	314	0.006	52333	-----
P5	34.17	31.29	636	-----	636	-----	-----	-----
P6	34.12	31.22	402	993	698	-----	-----	-----
P7	34.14	31.25	346	610	478	-----	-----	-----
P8	34.17	31.25	564	-----	564	-----	-----	-----
P9	34.19	31.27	303	893	598	-----	-----	-----
P10	34.22	31.28	464	-----	464	0.02	23200	-----
P11	33.85	31.04	979	1000	990	0.059	16780	-----
P12	33.82	31.13	868	-----	868	-----	-----	-----
P13	33.81	31.12	1185	-----	1185	-----	-----	-----
P14	34.11	31.24	155	144	149.5	0.096	1563	-----
P15	34.12	31.23	688	702	696	0.014	49714	-----
P16	34.13	31.26	395	479	437	-----	-----	-----
P17	34.17	31.28	453	800	627	-----	-----	-----
P18	34.18	31.28	564	706	635	-----	-----	-----
P19	34.19	31.28	1013	693	853	-----	-----	-----
P20	34.19	31.29	724	828	776	-----	-----	-----
P21	34.21	31.30	1199	1318	1259	-----	-----	-----
P22	34.21	31.30	117	182	149.5	-----	-----	-----

QANSA from rainfall was estimated from the calculated soil infiltration rate (Table 2) resulted from the data analysis of the three performed double ring infiltration tests as described by [25]. The field data were analyzed according to [26] equations:

$$D = Sp\ t^{0.5} + k\ t \quad (1)$$

$$I = 0.5\ Sp\ t^{-0.5} + k \quad (2)$$

where, D is cumulative infiltration (L), t is elapsed time (T), Sp is the sorpitivity, k is the soil parameter related to hydraulic conductivity of saturated soil (LT^{-1}) and I is the soil infiltration rate (LT^{-1}). The net recharge from rainfall (Fig. 7) was estimated applying the following relation [27]:

$$R = f * A * \text{Normal rainfall in monsoon season} \quad (3)$$

where, f is the rainfall infiltration factor (dimensionless), A is the area occupied by the formation (L^2), (the areas where the slope is more than 20% were excluded), R is the groundwater recharge from rainfall (L^3T^{-1}).

In addition, the western part of the QANSA capacity was estimated through carrying out three pumping and recovery tests and the data were analyzed applying [28] straight line method. The results were given in Table 2.

In the other side, the methodological approach used in this paper for groundwater flow simulation is based on the mathematical modeling techniques applying FEFLOW software (FEFLOW v.5.1, 2004). FEFLOW is a 3D finite element based groundwater simulation system capable of modeling time-dependent flow as well as mass transport problems. The time-dependent data that should be included into the FEM model has to be stored outside in database or GIS systems. The model describes groundwater flow of constant density under non-equilibrium conditions in a heterogeneous and anisotropic medium based onthe following equation [29].

$$\frac{\partial}{\partial x}[T_{xx}\frac{\partial H}{\partial x}] + \frac{\partial}{\partial y}[T_{yy}\frac{\partial H}{\partial y}] + \frac{\partial}{\partial z}[T_{ZZ}\frac{\partial H}{\partial z}] = S\frac{\partial H}{\partial t} + W + \sum_{k=1}^{m}[\delta(x - x_k).\delta(y - y_k).Q_k] \quad (4)$$

where; T_{xx}, T_{yy} & T_{zz} are the transmissivity in the x,y, & z direction (L^2/T), H, is the potentiometric head (L), S is the storage coefficient (dimensionless), W is the distributed volumetric water flux per unit area, positive sign for discharge and negative sign for recharge (L/T), Q_k is the volumetric water flux at point (source/sink) located at (x_k, y_k), positive sign for withdrawal and negative sign for injection (L^3/T), $\delta(x - \xi)$ is the Dirac delta function, t is the time (T), x, y are the Cartesian coordinates in the principal direction of transmissivity (L), m is the number of nodal points.

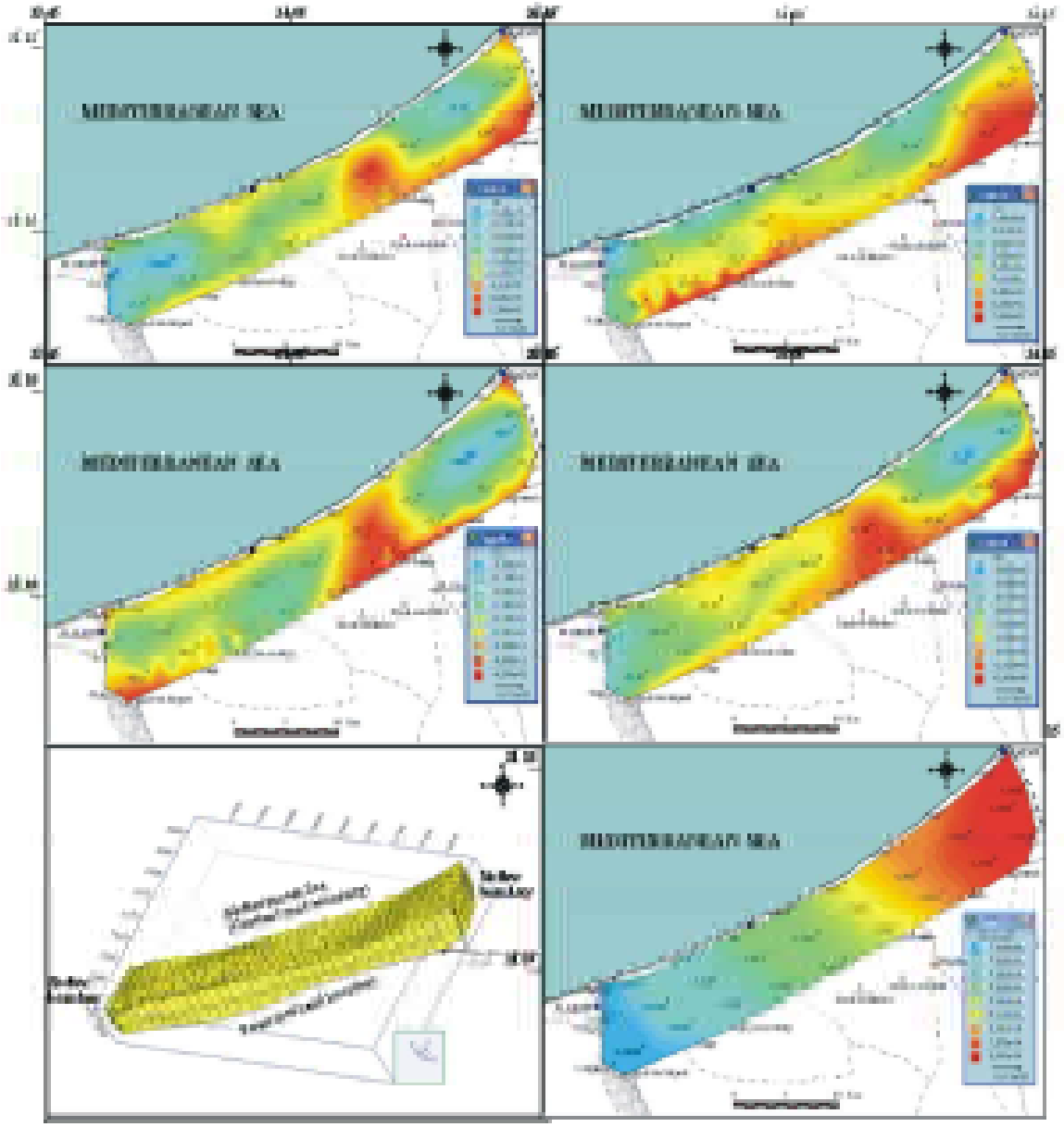

Fig. 7: Holocene top elevation slice (upper right) and bottom elevation slice (upper left), Kurkar top elevation slice (middle right) and bottom elevation slice (middle left), the finite element mesh of the eastern part of QANSA (lower left) and the aquifer net recharge rate (x10-4 m/day-lower right)

This equation was solved using the Adams-Bashforth/Trapezoid rule (AB/TR) predictor-corrector time stepping scheme and best-accurate Galerkin-based formulation no upwinding method and the finite element technique [30]. Characteristics of the groundwater flow mechanism and its spatial and temporal variation, as well as its future behavior, were thoroughly investigated by means of the mentioned numerical model.

Construction of the Groundwater Flow Model: The construction of the groundwater flow model of the QANSA required the definition of the conceptual model, the model domain with flow boundary conditions and the aquifer material properties.

Conceptual Model: The conceptual model of the eastern part of QANSA was based on the geology of the study area. The hydrogeological system was concerned two

hydraulically connected water bearing formations. The top hydrostratigraphic unit (Holocene sand dunes) was considered to be a sandy unconfined aquifer zone up to 30 m maximum thick. The second aquifer zone (Kurkar Formation), located below the sandy unconfined aquifer zone and had maximum thickness of 70 m. The scattered new communities around the asphaltic road in the E-W direction of the El-Arish-Rafah area were primarily planned for agriculture.

Model Mesh System and Boundary Conditions: The model domain with flow boundary conditions were chosen to cover an area of 600 km^2. Accordingly, the 6–nodal triangular prism mesh designed for the mathematical model in El Arish-Rafah area (eastern part of QANSA) consists in plain view of 1197 elements and 968 nodes (Fig. 7). Furthermore, FEFLOW's finite element allows performing local mesh refinements only in the areas of interest where enough hydrogeological data and realistic spatial distribution of required extractions are available. The two aquifer zones were discretized into 2 layers and 3 slices (Fig. 7). Ground elevation slice with 320256 ground elevation data sets extracted from DEM, Holocene Formation bottom level slice, Kurkar Formation top and bottom level slices (Fig. 7).

The hydraulic conditions at the boundaries of the model domain were specified. The northern boundary is defined by the sea water level (zero level) and is simulated as a fixed head boundary.

$$\frac{\partial}{\partial x}[Dx\frac{\partial C}{\partial x}]+\frac{\partial}{\partial Z}[Dz\frac{\partial C}{\partial Z}]-\frac{\partial}{\partial x}(Cv_x)-\frac{\partial}{\partial Z}(Cv_z)-\frac{C_oW}{nb}+\Sigma R_k=\frac{\partial C}{\partial t}\left(1+\frac{\rho_b}{n}K_d\right) \quad (5)$$

While the southern boundary is defined by the inflow front to the El Arish-Rafah area and is modeled as specified head boundary (6 m asl). Moreover, the eastern and the western boundaries were considered no flow boundaries. The upper boundary is defined by the altitude of the top surface of the Kurkar aquifer. The lower boundary is defined by the shape of the impermeable bed surface. The entry of this boundary is the absolute impermeable bed elevation at the different nodes of the model mesh. The FEFLOW computer code uses these values of the aquifer lower and upper boundaries to calculate the aquifer thickness for each element node.

Aquifer Hydraulic Properties: The QANSA characteristics required for simulation process include hydraulic conductivity and storage coefficient. In the model domain, the hydraulic conductivity values vary from $0.0072x10^{-4}$ to $0.051x10^{-4}$ m/sec in upper layer (Holocene layer) and between $0.062x10^{-4}$ to $0.43x10^{-4}$ m/sec for Kurkar layer. These values give a relatively better approximation of the field measurements (Fig. 8). The northeastern region adjacent to Rafah front shows high values of hydraulic conductivity and thus considers as a good prospects for drilling wells with high extraction rates.

In addition, the storage coefficient distribution map was drawn (Fig. 8). From this map it is noticed that, the estimated storage coefficient values in the model domain are closely related to the values measured in the field (ranges from 0.011 at the south to 0.066 at Al Arish area). Furthermore, the model domain as a whole has relatively high storage coefficient values and thus the eastern part of the QANSA should be treated as one layer of unconfined condition.

In addition, characteristics of the seawater intrusion mechanism and its spatial and temporal variation, as well as its future behavior, are thoroughly investigated by means of the 2D-SINM subroutine code [31]. It is utilized to incorporate the diffusion and hydrodynamic dispersion mechanisms into the simulation domain. This two-dimensional finite element model is based upon a velocity dependent dispersion coefficient [31]. The equation describing the transport in the two-dimensional model, which includes advection, dispersion and adsorption, is written as [29]. Where° Dx, Dz are the dispersion coefficients in x, z directions ($L^2 T^{-1}$). C is the concentration of the solute (ML^{-3}).vx, vz are the seepage velocity (LT^{-1}). C_o is the solute concentration in source or sink fluid (ML^{-3}). W is the source or sink term (LT^{-1}). n is the effective porosity. B is the aquifer thickness (L). R_k is the rate of addition or removal of solute ($ML^{-3}T^{-1}$). t is time (T). ρ_b is The bulk dry mass density (ML^{-3}). K_d is the distribution coefficient (L^3M^{-1}).

In this model, the modified 6-node bi-linear triangular finite elements are used to solve numerically the governing equations using Gauss-Siedel iteration method. The study domain is 10 Km in length (El-Arish sea-coast along the Y-direction with zero values for X-coordinate) and 18 Km in Delta Wadi El-Arish inland length (X-direction) with total surface area of 180 Km^2. The computational grid for the domain of Delta Wadi El-Arish is divided into 90 rows and 50 columns of triangular finite elements (Fig. 9). Vertical homogeneity is assumed adequate to allow treatment as a single layer with a mean hydraulic conductivity of 14 m/day. Longitudinal and lateral dispersivities are set equal to 10 m and 1 m, respectively. The effective porosity is set equal to 7%

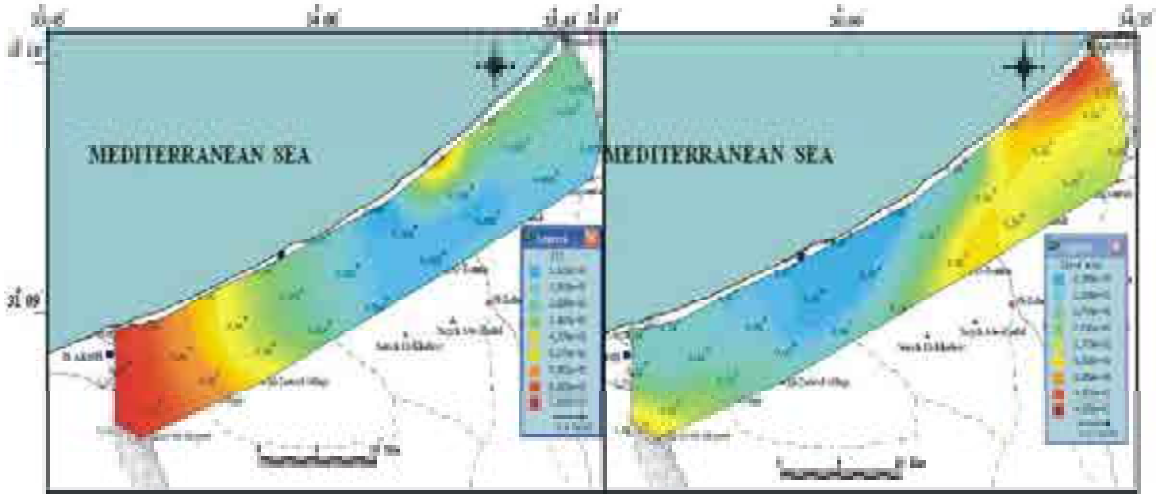

Fig. 8: The hydraulic conductivity distribution map (right map) and the storage coefficient distribution map (left map) of the model domain

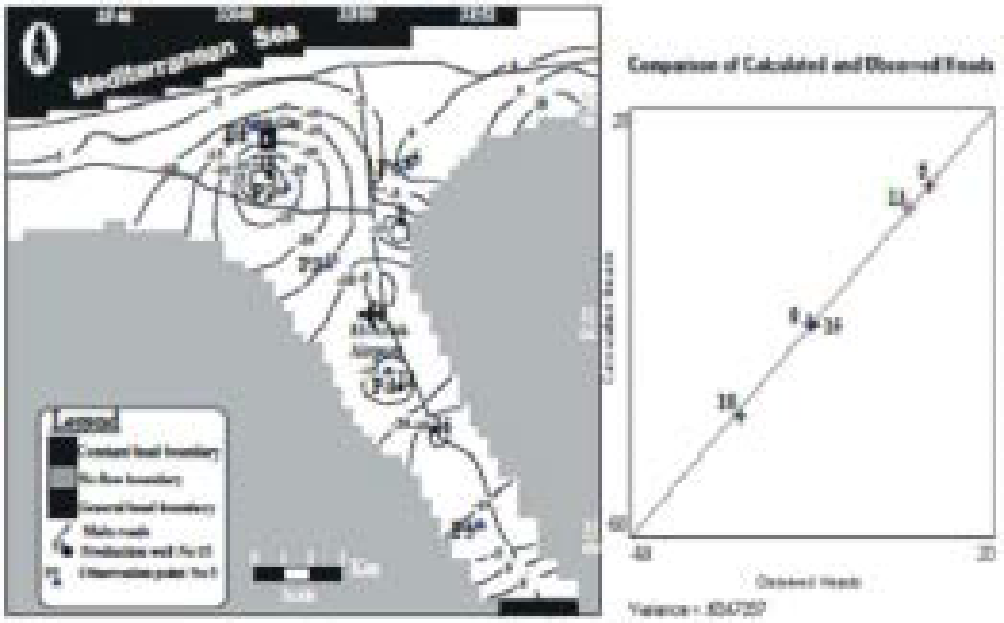

Fig. 9: The location of observation points and calibration results of seawater intrusion simulation applying MODFLOW and SINM models

Table 3: The testing scenarios for predicting the seawater intrusion in the eastern part of QANSA

Aquifer zone	Observation wells	Present conditions		Additional extraction						Scenario 4	
				Scenario 1 (8.25×10^6 m^3)		Scenario 2 (9.5×10^6 m^3)		Scenario 3 (8.75×10^6 m^3)		Sea water rise by 0.5 m	
		After 10 years	After 15 years	After 10 years	After 15 years	After 10 years	After 15 years	After 10 years	After 15 years	After 10 years	After 15 years
Coastal zone	P1	1.05	1.60	1.05	1.60	1.05	1.60	1.05	1.60	1.21	1.65
	P2	2.48	3.7	2.48	3.7	2.48	3.7	2.48	3.7	2.59	3.75
	P6	2.91	3.75	2.91	3.75	2.91	3.75	2.91	3.75	2.97	4
Airport zone	P3	4.14	6.21	4.14	6.21	10.27	15.4	16.24	24.37	4.14	6.21
	P4	4.97	7.45	4.97	7.45	12.31	18.45	19.48	29.18	4.97	7.45
Southern zone	P5	2.12	3.17	7.91	11.85	7.91	11.85	7.91	11.85	2.12	3.18

(average specific yield 7%). The northern boundary is saline sea-water transport boundary (35 g/l) since the QANSA was in direct hydraulic contact with the Mediterranean Sea in which the water level is known (zero). In the southern boundary, the salinity is assumed to be fixed (5 g/l) and the groundwater level reaches 8 m asl. The groundwater salinity ranges between 5 g/l and 2 g/l above datum on the eastern and the western sides, respectively. For the upper boundary, the water-table is considered higher than the Mediterranean Sea water level. The concentration is supposed to be constant and equal to the groundwater concentration. The bottom boundary is impermeable, i.e.; the normal flux through the bed for both fluid and salts is equal to zero.

Testing Scenarios: After completing the stage of calibration, the output of the first round is used to replace the initial condition with the condition of implementing the exploitation policies. The testing scenarios include three proposed water exploitation policies. The first scenario keeps the present extraction rate (52.2 million m^3/year at Sep. 2006) from the present cultivated areas without change. The second scenario assumes the decreasing of well discharge to the half through maximizing the use of surface runoff component via a system of earth dams and cisterns. The third scenario presumes an additional extraction of 8 million m^3/year (15% of the present annual extraction) to cover the new reclamation lands in Asser and Al Quareer area as impious governmental plan. The effect of these scenarios on the heads and groundwater flow directions of the eastern part of QANSA are shown.

In addition, the testing scenarios related to seawater intrusion are completely different. Under the present annual pumping rate of 19 million cubic meters (MCM), three proposed pumping scenarios are simulated based on the potentiality of QANSA to examine the impact on the seawater intrusion. The first scenario considers an annual increase in the pumping rate by 0.25 MCM (1.3% of the present discharge) from the southern zone of QANSA as a result of new agricultural activities (Table 3). For the second scenario, beside the extra 0.25 MCM from the southern zone, an additional 1.3 % of the present discharge is pumped from the middle zone (airport locality) due to drought cycle. Accordingly, the total additional extraction reaches 0.5 MCM from the model domain. The third scenario accounts for increasing the annual pumping rate from the middle zone by an additional 0.25 MCM for increasing population. With the third scenario, the total annual extraction rate from the QANSA reaches 19.75 MCM. The fourth scenario examines the effect of climatic change on seawater intrusion assuming a rise of sea water level by 0.5 m. A summary of the proposed additional extraction for the three scenarios is shown in Table 3. For the coastal zone of QANSA, groundwater extraction did not change during the proposed scenarios. To analyze the aquifer response to seawater intrusion under the three proposed scenarios, six observation points are selected as shown in (Fig. 9) to represent the overall aquifer zones. Observation points P1, P2 and P6 represent the northern part of the QANSA (the coastal area) where most of the pumping wells are concentrated and excess groundwater pumping is prohibited in this zone. Observation points P3 and P4 are located in El-Arish airport area, just close to the toe of the assumed sharp interface and drawdown is not allowed to keep the sharp interface at its current position. The last observation point P5 is located far from the deteriorated areas (the southern part of the QANSA) and sharp drawdown is not allowed to avoid the undesirable seawater intrusion.

RESULTS AND DISCUSSION

The analyzed data of the infiltration tests (Table 2) show that the infiltration rate ranges between 10.44 m/day and 26.06 m/day, while the sorpitivity varies from 0.437 $cm/min^{0.5}$ and 1.89 $cm/min^{0.5}$. According to Kohnke classification [32], the investigated soils vary from slow to rapid categories. In addition, the resulted data from the pumping tests analysis show that the transmissivity of the QANSA ranges from 149.5 to 1259 m^2/day and the storativity coefficient from 0.006 to 0.069. The diffusivity (T/S), which expresses the QANSA potentiality, ranges from 1563 to 52333 m^2/day (well No. P14 in the middle of Delta Wadi El-Arish and well No. P4 in the northern part of Delta Wadi El-Arish respectively, Table 2). This indicates that the eastern part of the QANSA has groundwater potentiality more than its value in the western part. Accordingly, the location of the wells in western part (Qatia and Gilbana localities) may not be in the proper site.

On the other hand, the results of the routine chemical analysis of the selected groundwater samples (TDS, Na and Cl in mg/l, Table 1 & Fig. 2) show little increase in groundwater salinity during the period 2006-08. While the long-term records (1962-2006) exhibit sharp increase in groundwater salinity (Fig. 6).

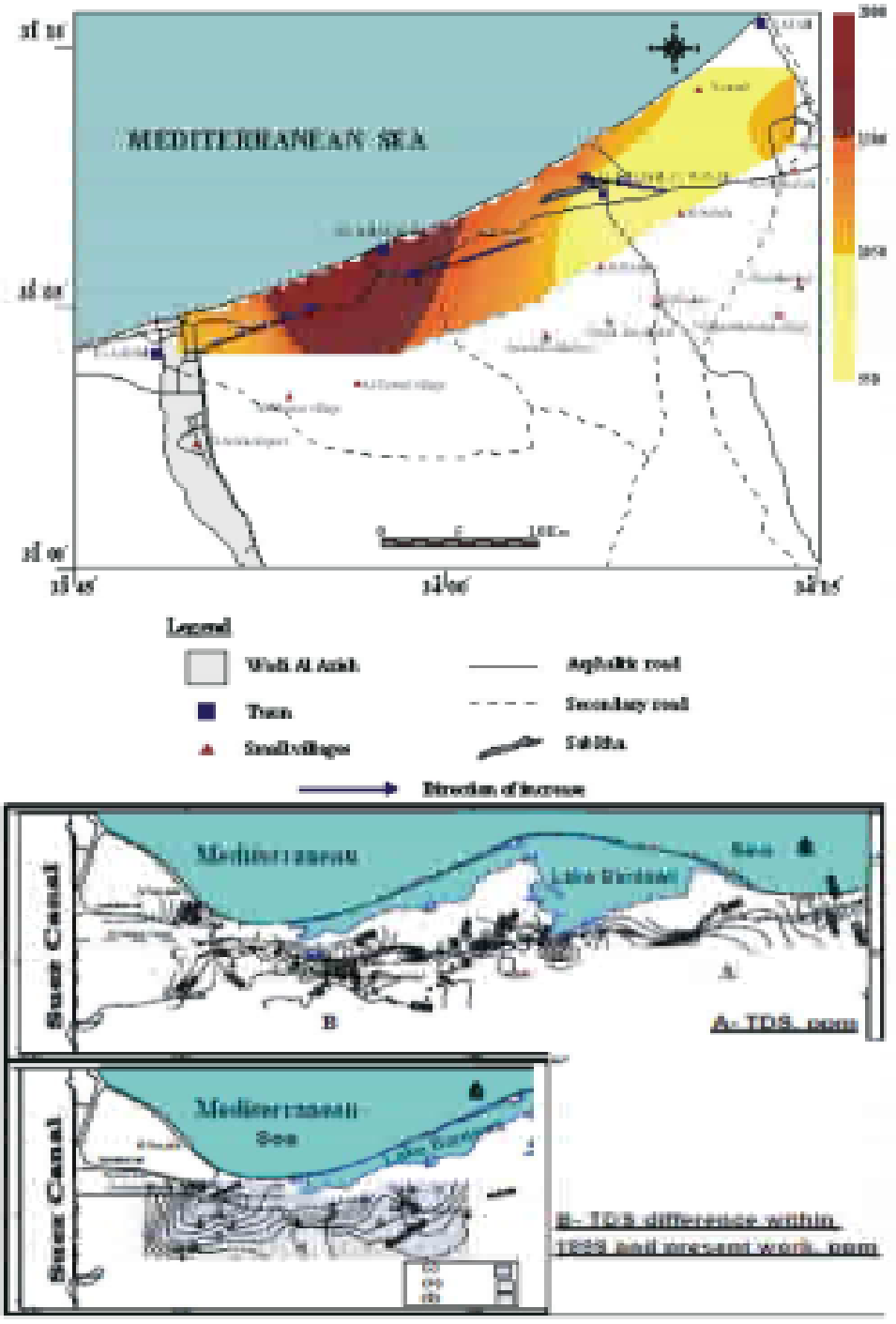

Fig. 10: Iso-salinity zonation map of the groundwater of the eastern part of QANSA (upper map) and western part (lower map)

As a general, the groundwater salinity of the eastern part of the QANSA ranges from 550 to 2000 mg/l as a result of over-pumping, particularly in the coastal and central parts (Fig. 10-upper map). This may accelerate seawater intrusion and cause continuous landward migration of toe. Based on the temporal salinity records, the migration of the toe changes from 2 to 5 Km inland [17, 18, 33] (Fig. 6).

In addition, the total dissolved solids (TDS) concentration of the western area of QANSA can be classified into three sub regions A, B and C (Fig. 10-lower map). The TDS concentration in sub region (A) is increased due north. It reflects the impact of seawater intrusion. The reverse trend is noticed around El Salam canal (sub area B), the TDS concentration is increased in the southern part. It is caused by dilution from El Salam canal. The exception for sub area B was noticed at Qatia and Gilbana. At Qatia, the TDS concentration is increased due north. This may attribute to presence of Holocene aquifer underlain by chalky limestone. At Gilbana, the TDS concentration is increased towards the southwestern part due to recharge from El Qantara canal (saline water). On the other hand, the TDS concentration is increased in the northwestern direction, i.e. towards the Suez canal in sub area C, which is caused by seawater encroachment of Suez canal.

The TDS concentration of the QANSA is controlled by the amount of rainfall, seawater intrusion, seepage from El Salam canal and the over exploitation activity. Nevertheless, salts evaporates, lithogenic source and evaporation process play an important role in the groundwater salinity particularly at the shallow depths. The difference between TDS concentration in 2000 and present work is estimated in zonation map (Fig. 10B).

In the other hand, the results of the simulation process of the eastern part of QANSA reveal that the implementation impacts of the proposed development policies have serious impacts on the QANSA storage. Figure 11 shows the predicted hydraulic head in the QANSA's drilled wells and water balance components after time of simulation of 20 years applying the different proposed scenarios.

It is noticed from the figure that, under the exploitation strategy of 52.2 million m^3/year (first proposed scenario), the total drawdown ranges from 5 m in the coastal area to 10 m in the central part of the modeled area between El-Arish and El-Kharouba (Fig. 11-upper). The lowering in the predicted hydraulic head drawdown in the southern part of the model domain compared with the other aquifer localities may be attributed to the increase in aquifer thickness, increase in sand ratio and high lineaments density due south. In addition, the predicted water balance components and the resulting head distribution map of this scenario after 20 years are plotted (Fig. 11-upper). From this figure, it seems that the predicted difference in Q_{TOTAL} indicates a loss in groundwater storage amount to 9230.57 m^3/day. It represents about 22% of the current discharge rate. This means that, at the end of simulation time (20 years) the discharge starts to diminish and as a result, the critical aquifer depletion wills exist. It is worth to mention that, the occurrence of cones of depression is expected within about the central cultivated area between El-Arish and El-Kharouba especially at the central part of the modeled area by the end of 20 years. This may attribute to the effect of numerous faults trending NE – SW and NW – SE directions, which throw towards the east-west and NE-SW respectively and resulted in decreasing the thickness of water bearing formation at these areas. The flow directions are mostly changed especially towards this part of the modeled area, which reflects more deterioration of this part. As a result of the above discussion of the aquifer response to the first extraction scenario, it can be concluded that the present groundwater withdrawal (52.2 million m^3/year) from the eastern part of QANSA could not be safely predicted. Accordingly, this situation is very critical and needs a new developed strategy as fast as possible.

In addition, the results of the simulation process applying the second proposed scenario (assuming a decrease in discharge rate to the half, i.e., about 26 million m^3/year) amount to groundwater levels increase in the most of the modeled area during the period of simulation. The predicted increase in groundwater level ranged from 5 min coastal area to 30 m in the central area between El-Arish and El-Kharouba while the increase of the initial water table to more than 20 m is pronounced in the Al-Maazar cultivated areas after the simulation time period. Moreover, the predicted water balance components and the resulting head distribution map of this scenario after 20 years are plotted (Fig. 11-middle). From this figure, the predicted difference in Q_{TOTAL} indicates a gain in groundwater storage by 2031.18 m^3/day. It represents about 45% of the total discharge rate. This means that, at the end of simulation time (20 years) the recharge to the aquifer from the adjacent aquifers will increase and consequently, the aquifer storage will increase. Also, the expected cones of depression due to the first proposed scenario is expected to disappear within about the central cultivated area between El-Arish and El-Kharouba especially at the central part of the modeled area by the end of 20 years [34]. Opposite to the second scenario, the third one assumes an increase in discharge rate by 20 % (about 10^4 m^3/day) which satisfies the irrigation water requirements of the new reclaimed area in Asser and El-Qawareer area

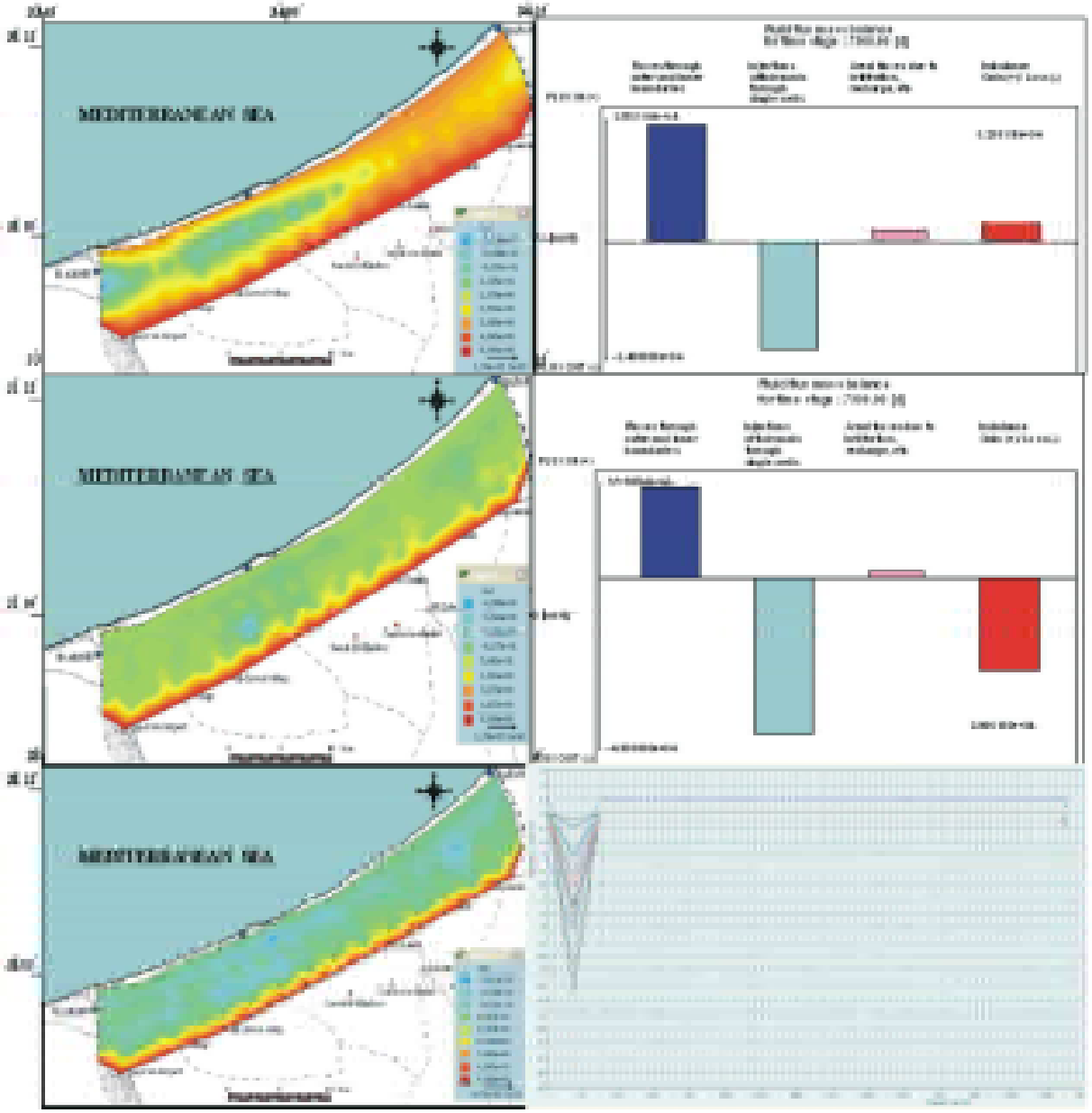

Fig. 11: Predicted head distribution map and predicted water balance components of the eastern part of QANSA applying [39] in case of 1st scenario (upper), 2nd scenario (middle) and 3rd scenario (lower)

SW the model domain. Spotlight on the head changes after the simulation time interval (20 years) shows that the groundwater levels are declined in the model domain from 4 m in the coastal area to 15 m in the central area between El-Arish and El-Kharouba. The decline of the initial water table to more than 15 m is pronounced in most of the southern villages and the depleted part of the aquifer saturated thickness will increase to more than 40% for most of the modeled area. Moreover, the basic components of the predicted water balance for the total modeled area and their corresponding estimated hydraulic head distribution map a fter 20 years are constructed (Fig. 11-lower). The difference between the groundwater input and output under this stress reached 20861.35 m^3/day. It denotes more than 50% of the total discharge rate from the reclamation areas. This may cause great deterioration and critical depletion problem due to the increase of the groundwater extraction from

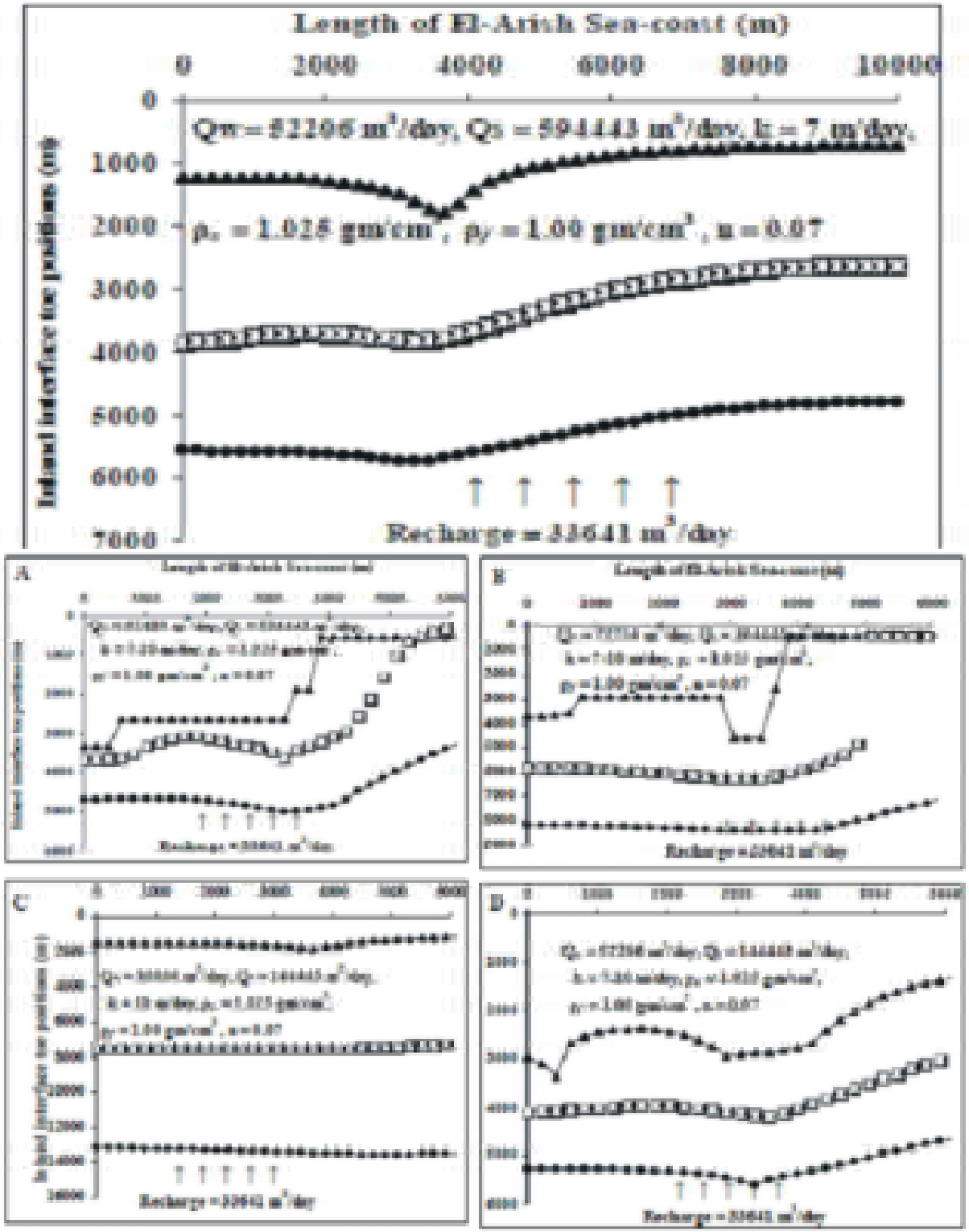

Fig. 12: The predicted inland interface toe positions from its initial position after 5 years (line with triangles), 10years (line with squares) and 15 years (line with circles) under the current state of pumping (upper chart), under 1st scenario (chart A), under 2nd scenario (chart B), under 3rd scenario (chart C) and under 4th scenario (chart D)

40000 to 49000 m^3/day as proposed in this scenario. Accordingly, the hydraulic gradient will increase in the modeled area in the end of the simulation period. As a result of the above discussion of the aquifer response to the third extraction scenario, it can be concluded that the reclamation activity at Asser and El-Quareer area needs surface water more than groundwater resources. Although the Egypt national security is in opposite direction with the extension of El-Salam canal to this area, the limitation of the groundwater resources propose searching for other water resources for sustainable development of this area.

As a result of the above discussion of the aquifer response to the proposed extraction scenarios, it can be concluded that the proposed groundwater withdrawal of 26 million m^3/year from the eastern part of the QANSA (the second proposed scenario) considers the optimal solution for the groundwater management problem in the study area [34].

Otherwise, the results of simulation of seawater intrusion applying the SINM code are given in (Fig. 12).

As mentioned before, the calibrated and predicted groundwater levels in the eastern part of QANSA resulted from MODFLOW model is applied as inputs for SINM model in order to predict the future behavior of the intrusion. The prediction of the interface toe positions under different stresses from pumping applying SINM model is determined (Table 3). A definition sketch of the studied domain including different data and the meaning of the parameters used in every case is related to these figures. SINM model outputs (Fig. 12) show the advancing of seawater intrusion in case of both the current and the proposed pumping stresses from 18 pumping well fields located at distance more than 2 Km from the coast. The current pumping stresses (Qw = 52206 m^3/day) will cause the intrusion to invade a distance of 1.2, 3.8 and 5.5 Km from its current position after 5, 10 and 15 years respectively (Fig. 12). In general, the advanced interface toe to the well field location goes to be undulated in all scenarios. This behavior may attribute to the increase in the local effect of every well field as the interface toe approaches to the well field location [35]. This undulation increases with increasing the spacing between wells [36, 37, 38]. So, the average location from the coast for interface toe at each row of nodes perpendicular to the coast for biggest well spacing is smaller than that for small spacing. This finding may help in decrease the intrusion of definite localities in the modeled area by choosing the proper well spacing. To catch the maximum allowable pumping rate from the model domain, the problem must be solved for different consecutive increasing rates of pumping with interval difference equal to 10 m^3/day till the well field system was polluted. In this analysis, the position of the interface toe under the proposed four scenarios reached 4.8 km, 8 km, 13 km and 5.3 km from its current position respectively after 15 years (Fig. 12). To control the seawater intrusion, the groundwater flow to the sea (Qs) will reach 534443, 394443, 144443 and 144443 m^3/day respectively after the same period of simulation (Fig. 12). The similarity between Qs due to 3rd and 4th scenarios reflects the negative impact of the climatic change on the groundwater resources management of the modeled area. In the other side, the shallow wells less than 30 m at distances of 11Km from the coast will polluted and the deeper wells will pump more saline water because of the rising of the sea water level. It is quite clear that present water production policies need to be modified otherwise the aquifer will be severely contaminated by progressive seawater intrusion.

CONCLUSION AND RECOMMENDATIONS

Numerical research is introduced in this paper to investigate the problem of groundwater management and seawater intrusion in salt-affected ecosystems of QANSA. The hydrogeological investigation of the QANSA reveals that the aquifer system is continuously replenished by the rainfall (10%) and subsurface flow (2 MCM). The transmissivity of the QANSA ranges from 208 to 468 m^2/day and 0.06 to 0.08 for specific yield. The historical and current hydrogeochemical analyses data show that there is a continuous increase in seawater intrusion.

Simulating the Kurkar aquifer (the eastern part of the QANSA) with suitable model provides proper utilization and good management of this aquifer. Finite Element Flow (FEFLOW) program is used for this purpose. A mesh of 1197 elements and 968 nodes is applied on the modeled area. Three management scenarios are proposed to examine the behavior of the aquifer under different stresses for 20 years of simulation time. The first scenario, assumes the present discharge rate (52.2 million m^3/year) from the cultivated areas. The results reveal a critical groundwater drawdown (10 m) due to the great amount of groundwater extracted from these areas. The second scenario, (promising extraction case), presumes the expected total amount of groundwater extractions (26 million m^3/year) from the cultivated areas, due to the maximizing of the surface runoff utility. Applying this plan, the maximum groundwater decline reaches 5 m. The

third scenario, assumes an increase in discharge due to the new reclamation projects by 20 % (about 10^4 m^3/day). The maximum decline in groundwater levels in El Sheikh Zuwayid area reaches 15 m for time interval of 20 years.

In addition, characteristics of the intrusion mechanism and its spatial and temporal variation, as well as its future behavior, are thoroughly investigated by means of two numerical models (MODFLOW and SINM codes). The two codes are used for definition of the flow mechanism and the initial conditions for flow and to simulate the QANSA under different operational scenarios. The second model (SINM), depending on the MODFLOW outputs, is applied for predicting the interface toe positions under the proposed scenarios. Three proposed pumping scenarios are assumed based on the potentiality of the model domain of the eastern part of QANSA to examine the impact on the seawater intrusion. The first scenario considers an annual increase in the pumping rate by 0.25 MCM from the southern zone of the model domain as a result of new agricultural activities, the second scenario assumes an additional annual increase in the pumping rate by 0.25 MCM from the middle zone, due to expected drought cycle, the third scenario accounts for increasing the annual pumping rate from the middle zone by an additional 0.25 MCM for increasing population and the fourth scenario examines the effect of climatic change on seawater intrusion assuming a rise of sea water level by 0.5 m. The position of the interface toe under these proposed four scenarios reaches 4.8 Km, 8 Km, 13 Km and 5.3 Km from its current position respectively after 15 years. To domesticate seawater intrusion, the groundwater flow to the sea may be greater than 144443 m^3/day and the discharge from the model domain should be properly managed. Migration rate of seawater intrusion may be reduced by thorough investigation and planning new management policies for optimal use the freshwater in the eastern part of QANSA. It is recommended to perform monthly or bi-monthly groundwater level and salinity measurements for better model calibration and verification. Testing different discharge-recharge cycles or extraction barrier to identify the best operation strategy is also needed.

REFERENCES

1. Wilson, J. and H. Guan, 2004. Mountain block hydrology and mountain front recharge. In: Hogan JF, Phillips FM, Scanlon BR (eds) Groundwater recharge in a desert environment: the southwestern United States. AGU, Washington, DC, pp: 113-137.
2 Williams, J., 2001b. Salt balance in the Rio Grande project from San Marcial, New Mexico, to Fort Quitman, Texas. M.Sc. Thesis, New Mexico State Universitry, Las Cruces, NM.
3. Jennifer, L., H. James, E. Christopher H. Barry and H. William, 2008. Hydrogeology controls on groundwater recharge and salinization: a geochemical analysis of the northern Hueco Bolson aquifer, Texas, USA. Hydrogeol. J., 16: 281-296.
4. Richter, B. and C. Kreeitler, 1993. Geochemical techniques for identifying sources of groundwater salinization. CRC, Boca raton, FL, pp: 258.
5. El-Said, M., 1994.Geochemistry of groundwater in the area between El Qantara and El Arish, North Sinai. Ph.D. Thesis, Fac. Sci., Ain Shams Univ., Cairo, Egypt.
6. Taha, A.M., 1968. Geology of the groundwater supplies of El Arish-Rafah area, northeast Sinai, U.A.R. M.Sc. Thesis, Fac. Sci., Cairo Univ., Egypt, pp: 129.
7. Shata, A.A., 1960. The geology and geomorphology of El- Qusayima area, northeast Sinai, Egypt. Bull. Soc. Geograph, Egypt, pp: 95-146.
8. Pavlov, H.L. and M. El Ayuti, 1961. Groundwater of the Sinai Peninsula. Bull. Inst. Desert, Egypt.
9. Said, R., (ed),1962. The geology of Egypt. Elsevier, the Netherlands, pp: 377.
10. El Shazly, E.M. M.A. Abdel-Hady, M.A. El Ghawaby, I.A. El Kassas and M.M El Shazly, 1974.Geology of Sinai Peninsula from ERTS-1 Satellite Images". Remote Sensing Research Project. Academy of Scientific Research and Technology, Cairo, Egypt.
11. Jenkins, D., J.C. Harms and T.W. Oesleby, 1982. Mesozoic sediments of Gebel Maghara, North Sinai, Arab Republic of Egypt. The 6th Exploration Seminar, E. G. P. Co. Cairo, Egypt, pp: 46.
12. El-Ghazawi, M.M., 1989. Hydro-geological studies inNorth East Sinai–Egypt. Unpublished Ph D Thesis, Fac. of Sci, El Mansoura University, pp: 290.
13. Said, R., (ed), 1990. The geology of Egypt. Balkema, A.A., Potterdam, Brookfield, the Netherlands, pp: 734.
14. Japan International Cooperation Agency (JICA), 1992. North Sinai groundwater resources study in the Arab Republic of Egypt. Final report submitted to the Research Institute for Water Resources, Water Research Center, Ministry of Public Works and Water Resources, Cairo, Egypt, pp: 214.
15. El-Osta, M., 2000. Hydrological studies on the area between El Qantara and Bir El Abd,North Sinai, Egypt. M.Sc. Thesis, Fac. Sci., Minufiya Univ., Cairo, Egypt.

16. Abd El-Aal, G., 1992. The ground water conditions in the area from Rommana to Bir El Abd, especially the area south of Rabaa Village, Northwestern Sinai Peninsula, A.R.E. M.Sc. Thesis, Geol. Dept., Fac, Sci., Cairo Univ., pp: 145.
17. Saad, K.F., 1962. Report on hydrology of groundwater in wadi El Arish, north Sinai, Egypt. Internal report, Desert Institute, Cairo, Egypt, pp: 36. (In Arabic).
18. Saad, K.F., I.Z. El Shamy and A.S. Sewidan, 1980. Quantitative analysis of the geomorphology and hydro- geology of Sinai Peninsula. The 5th conference on African geology, Cairo, Egypt, pp: 19.
19. Eweida, E.A., 1993. Effect of rainfall and runoff on the flushing groundwater in Wadi El Arish delta, Sinai, Egypt. Science, Monthly Magazine, Water Research Center, Water Science, 13: 12-18.
20. Rizk, Z.S., I.Z. El Shamy, S. Zaghloul and A.S. Seleem, 1995. Prediction of salt-water intrusion at El-Arish-Rafah area. Proc. 4th Canf. Geol. Sinai Develop., Ismailia, pp: 171-188.
21. GAD, M.I., A.E.A. El Sheikh and M.S. El Maghraby, 2009. Application of mathematical modeling in the study of sea water intrusion in the coastal quaternary aquifer, Delta Wadi El Arish, Egypt. Egyptian Journal of Aquatic Research, 2009, 35(2): 69-85.
22. Helwa, M., 1993. Sinai water resources maps. Final internal report to WRRI, Cairo, Egypt, pp: 191.
23. Dames and Moore, 1981. Agricultural and water investigations of Sinai. Phase 1, part 1(136p.) and part 11(44p.), final report performed by the Desert Institute and submitted to the Advisory Committee for Reconst- ruction, Ministry of Dev. and New Commun., Arab Republic of Egypt.
24. Ghodeif, K. and M.H. Geriesh, 2006. Contamination of domestic ground- water supply of El-Arish City, North Sinai, Egypt. Proc. 7th Conf. Geol. Sinai Dev., Ismailia, pp: 171-188.
25. Black C., 1973. Methods of soil Analysis. Am. Soc. Agron. Inc. Publ, Madison, pp: 137.
26. Philip, J.R., 1957a. The theory of infiltration 1. The infiltration equation and its solution. Soil Sci., 83: 345-357.
27. Raghunath, H.M., 1997. Hydrology. Principles. Analysis. Design. New Age International (P) Limited, Publishers, India, pp: 486.
28. Bear, J., 1979. Hydraulics of ground- water." McGraw-Hill, New York.
29. Warner, J., 1987. Mathematical Development of the Colorado State University Finite Element 2-Dimensional Groundwater Flow Model. Groundwater Technical Report 2, Colorado, USA.
30. Abdel-Gawad, H.A., 2004. Multi-objective management of hetero-geneous coastal aquifer. Mansoura Engineering Journal, 29(4): 1-14.
31. Kohnke, H., 1980. Soil Physics. Soil Scientists Purdue University, TATA Nc Grow-Hill Publishing Company LTD, New Delhi, pp: 28-34.
32. El Tablawi, E.M.S., 1997. Sea water intrusion in the coastal aquifer between Rafah and El Sheikh Zuwayid, North Sinai and its impact on the surrounding environment. M.Sc. Thesis, National and Biological Science Department, Institute of Environmental Studies and Research, Ain Shams University, Cairo, Egypt, pp: 198.
33. Sleem, M.A., 2009. Hydrological study on the Quaternary aquifer in El-Arish-Rafah area, Sinai peninsula-Egypt" Unpublished M. Sc. Thesis, Fac., Sci., Al-Azhar Univ., Asuit Branch, pp: 244.
34. El-Ghandour, H.A.A., 2005. Analysis and optimization of saltwater intrusion in coastal aquifers. Ph.D. Thesis, Fac. of Eng., El-Mansoura Univ., Irrig.,and Hydraulic Dept., pp: 161.
35. Mahesha, A., 1996. Steady-state effect of fresh water injection on sea water intrusion. Journal of Irrig. and Drainage Engineering, ASCE, 122(5): 266-271.
36. Saafan, T.A., 1995. Mathematical solution of sea water intrusion into fresh water in unconfined coastal aquifers. 5th Int., Conf., "Environmental Protection is A must Must", Apr. 1995, Alex., pp. 497-509.
37. Zhou, X., M. Chen, X. Ju, X. Ning and J. Wang, 2000. Numerical simulation of sea water intrusion near Beihai, China. Enviro. Geology, 40(1-2): 223-233.
38. El-Kashouty, M., M.H. El-Sayed, Y. Godamy, M. GAD and M. Mansour, 2012. Characterization of the aquifer system in the northern Sinai Peninsula, Egypt. Journal of Environmental Chemistry and Ecotoxicology, 4(3): 41-63.
39. FEFLOW v.5.301 software (2007) FEFLOW Interactive Graphics-based Finite Element Simulation System for Subsurface Flow and Transport Processes Copyright (c) 1979-2007 by WASY GmbH v. 5.301 (3D + 2D) (2007): WASY Institute for Water Resources Planning and Systems research GmbH. Watersdorfer Str. 105, D-12526 Berlin-Bohnsdorf, Germany. World Wide Web: http://www.wasy.de.